Progress In Electromagnetics Research Letters, Vol. 77, 35–40, 2018

A Ultra Compact Wideband Bandpass Filter Using a Quadmode Stub-Loaded Resonator

Zhi-Chong Zhang[1, *] and Hai-Wen Liu[2]

Abstract—An ultra compact microstrip wideband bandpass filter (BPF) using a quadmode stub-loaded resonator is presented in this letter. The resonant characteristics of the quadmode resonator are explored by adopting odd- and even-mode analysis. The four resonant frequencies of this resonator can be controlled independently. For demonstration purpose, a wideband BPF is designed, fabricated and measured. The measured results are in good agreement with the full-wave simulation results. The realized wideband filter exhibits a 3 dB fractional bandwidth (FBW) of 45% with good in-band filtering performance and sharp out-of-band rejection skirt.

1. INTRODUCTION

Wideband applications are becoming more and more widely used in modem wireless communication systems. So far, as an intensively studied topic, there are several approaches reported in the literature to design integrated wideband BPFs [1–12]. In [1], a lowpass filter and highpass filter in a cascade connection are used to design a wideband filter, and wideband BPFs using this kind of method have relatively large circuit size. In [2], a compact microstrip wideband BPF based on a square ring loaded resonator (SRLR) is proposed, which is formed by loading a pair of bent open-stubs outside the diagonal corners of a square ring, which generates three split degenerated modes. In [3, 4], a method of signal interaction of two transmission paths is employed to design a wideband filter, and wideband BPFs using this kind of method have relatively broader bandwidth and better selectivity, but the design processes are relatively complex. Finally, wideband BPFs are realized with the stepped impedance resonators (SIRs) [5–7] and stub loaded resonators (SLRs) [8–12] due to their multi-mode behavior. In [7], an improved quad-mode resonator and a coupled-line section are adopted to achieve a wideband filter with 88% (2.1 to 5.4 GHz) relative bandwidth. In [8], two multiple-resonance microstrip ring resonators with loading of open-circuited stubs are adopted to achieve a compact wideband bandpass filter with good out-of-band performance and sharpened rejection skirts. The stub is used to achieve multimode operation and additional zero point simultaneously in [9]. A novel wideband BPF based on a single slotline ring resonator with two dissimilar slotline stubs is proposed in [10]. A novel compact wideband BPF is proposed using quadmode resonator formed by attaching a short-circuited stub at the center plane and two identical impedance-stepped open stubs to high impedance microstrip line in [11]. A very broad stopband can be achieved in a triple-mode wideband BPF in [12]. Wideband BPFs using SIRs or SLRs have relatively simple design procedure and compact circuit size.

In this letter, wideband performance is realized by using a quadmode stub-loaded resonator, which has ultra compact size and controllable quadmode wideband performance. According to the even- and odd-mode method, the resonant frequencies of the first four modes for the resonator can be freely adjusted by controlling the corresponding dimension parameters. For demonstration, the proposed

Received 29 April 2018, Accepted 21 June 2018, Scheduled 28 June 2018

* Corresponding author: Zhi-Chong Zhang (z.zhichong@jgsu.edu.cn).

[1] College of Electronic and Information Engineering, Jinggangshan University, Ji'an 343009, China. [2] College of Information Engineering, East China of Jiaotong University, Nanchang 330013, China.

wideband filter is designed, fabricated and measured. The measured results are in good agreement with simulated predictions.

2. FILTER DESIGN

Quadmode stub-loaded resonator: Figure 1(a) shows the proposed quadmode resonator, which is composed by a dualmode open-loop resonator and two open stubs that are loaded at the open-loop. The total length of the two open stubs is L_1, which is equal to the total length from loading point to open-end of the dualmode open-loop. In addition, there is coupling between the two open stubs, and the coupling capacitor is C_1, which is equal to the self coupling capacitor of the open-loop resonator. Since the quadmode resonator is symmetrical to the dashed line, its resonant characteristics can be examined by the even- and odd-mode method [13]. The equivalent circuits of odd-mode and even-mode are depicted in Figures 1(b) and (c), respectively.

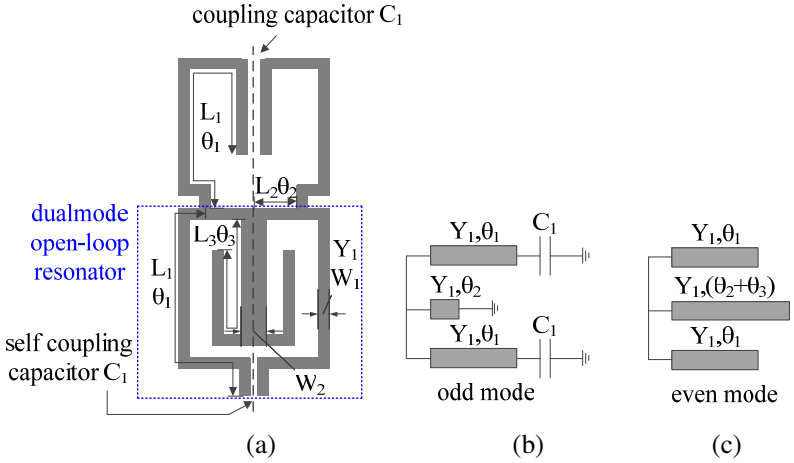

Figure 1. Structure and equivalent circuit of the proposed resonator. (a) Layout of the proposed resonator. (b) Odd-mode equivalent circuit. (c) Even-mode equivalent circuit.

Since the equivalent circuits of odd mode and even mode are also symmetric structures, the even- and odd-mode method is utilized again. The equivalent circuits of the quadmode are shown in Figures 2(a), (b), (c) and (d), these resonant conditions can be derived as

$$\cot\theta_{1(\text{mode1})} = 0 \tag{1}$$

$$\omega_{(\text{mode2})}C_1 + Y_1\tan\theta_{1(\text{mode2})} = 0 \tag{2}$$

$$\omega_{(\text{mode3})}C_1 + Y_1\tan\theta_{1(\text{mode3})} + \frac{Y_1\tan\theta_{2(\text{mode3})}}{2} = 0 \tag{3}$$

$$\frac{\tan[\theta_{2(\text{mode4})} + \theta_{3(\text{mode4})}]}{2} + \tan\theta_{1(\text{mode4})} = 0 \tag{4}$$

where ω is the frequency in radians per second, and Y_1 is the characteristic admittance of the width W_1 of transmission line. θ_1, θ_2, and θ_3 denote the electrical lengths of L_1, L_2, and L_3 of transmission line. Subscripts (mode n) represent the quadmode resonator working at mode n. From Eq. (1), it can be seen that the resonant frequency of mode1 f_{mode1} can be determined by $\theta_1(L_1)$. Similarly, from Eq. (2) the resonant frequency of mode3 f_{mode2} can be decided by $\theta_1(L_1)$, $Y_1(W_1)$, and C_1. From Eq. (3) the resonant frequency of mode4 f_{mode3} can be decided by $\theta_1(L_1)$, $\theta_2(L_2)$, $Y_1(W_1)$, and C_1. From (4) the resonant frequency of mode2 f_{mode4} can be decided by $\theta_1(L_1)$, $\theta_2(L_2)$, and $\theta_3(L_3)$. For demonstration, we use a commercially available full-wave electromagnetic (EM) simulator ADS 2013. The design process of the quadmode stub-loaded resonator is depicted in Figures 3(a), (b), (c) and (d). First, determine the length of L_1 by f_{mode1} for the half wavelength resonator in Figure 3(a). Secondly, fix the value of

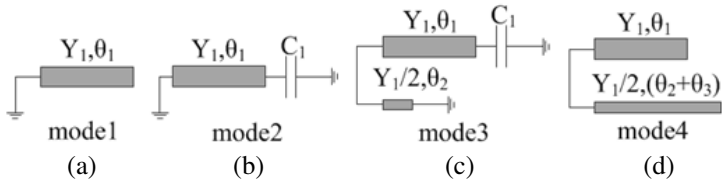

Figure 2. Equivalent circuits of the quadmode. (a) Mode 1. (b) Mode 2. (c) Mode 3. (d) Mode 4.

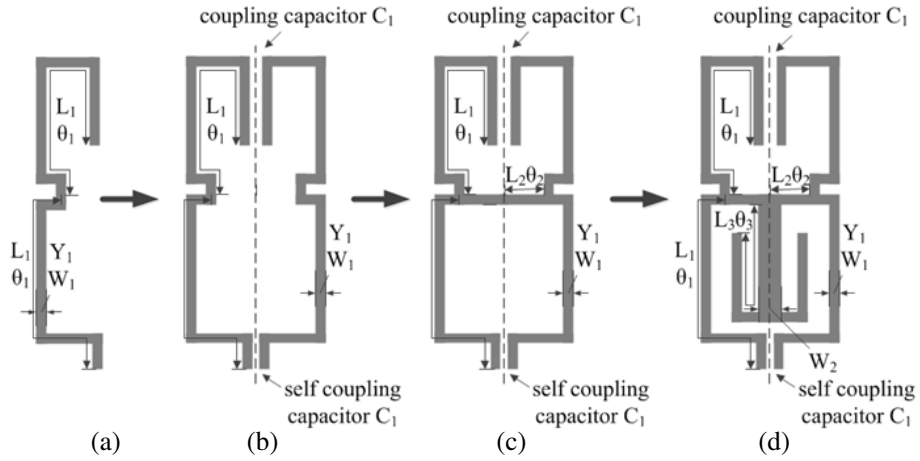

Figure 3. Design process of the quadmode stub-loaded resonator. (a) Half wavelength resonator. (b) A pair of coupled half wavelength resonators. (c) A pair of coupled half wavelength resonators with symmetrically centred points connected. (d) Quadmode stub-loaded resonator.

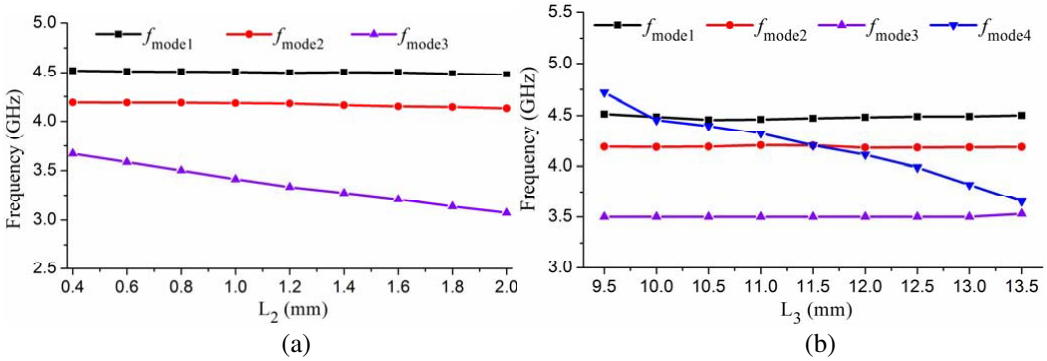

Figure 4. (a) Resonator characteristics of the resonator in Figure 3(c) with varied length L_2 under weak coupling. (b) Resonator characteristics of the quadmode resonator with varied stub length L_3 under weak coupling.

C_1 by f_{mode2} for the resonator in Figure 3(b). Thirdly, determine the length of L_2 by f_{mode3} for the resonator in Figure 3(c). Finally, fix the total length of L_3 by f_{mode4} for the quadmode stub-loaded resonator in Figure 3(d).

Obviously, the resonant frequencies f_{mode1} and f_{mode2} can be achieved by L_1 and C_1. Fix L_1 and C_1, Figure 4(a) is the extracted resonator characteristics of the resonator in Figure 3(c) with varied total physical length of L_2. As L_2 increases from 0.4 mm to 2 mm, the resonant frequency f_{mode3} shifts down toward lower frequency, while the resonant frequencies of f_{mode1} and f_{mode2} are nearly unchanged, which illustrates that the resonant frequency f_{mode3} can be controlled by L_2 independently. Figure 4(b) is the extracted resonator characteristics of quadmode stub-loaded resonator with varied physical length

of the loading stub L_3. As L_3 increases from 9.5 mm to 13.5 mm, the resonant frequency f_{mode4} shifts down, while the other mode resonant frequencies are nearly unchanged. It is noted that the resonant frequency f_{mode3} can be independently controlled by L_3.

To verify the applications to wideband BPF, the filter is designed with the following specifications: the center frequency f_0 =4 GHz and 3-dB fractional bandwidth FBW = 44%. The first four modes of the quadmode resonator are 3.5 GHz, 3.9 GHz, 4.1 GHz, and 4.5 GHz, successively. The simulated S_{21}-magnitude of the quadmode resonator to achieve wideband BPF under weak coupling is shown in Figure 5. The first four modes of the proposed resonator are combined to realize the wideband passband performance, and the FBW of the passband is decided by the resonant frequencies of the first four modes. The first high order mode appears at 8.6 GHz, which provides a wide upper stopband. Finally, by applying a feed structure with tight coupling strength to the proposed resonator, the wideband BPF is realized.

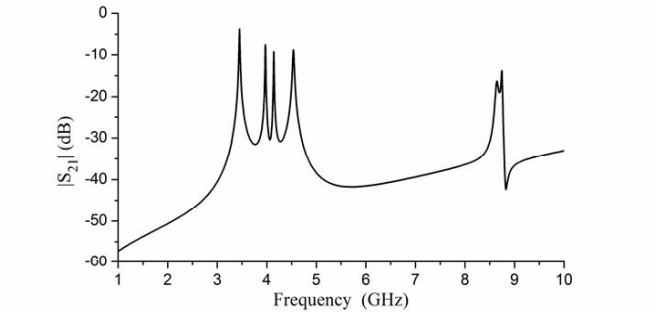

Figure 5. Simulated S_{21}-magnitude of the proposed quadmode resonator to achieve wideband BPF under weak coupling.

3. RESULTS AND DISCUSSION

Figure 6(a) shows the layout of the wideband microstrip BPF, which is designed and fabricated on a substrate having a thickness of 0.8 mm, relative dielectric constant of 2.55, and loss tangent $\delta = 0.0029$. This filter structure has an advantage of easy fabrication for no via-hole or aperture-back.

A photograph of the fabricated filter is shown in Figure 6(b). The size of the filter circuit is $18 \times 6\,\text{mm}^2$ ($0.3\lambda_g \times 0.1\lambda_g$, λ_g is the guided wavelength on the substrate at the center frequency of the passband). The bent structure with self-coupling is used to realize ultra compact size. The physical

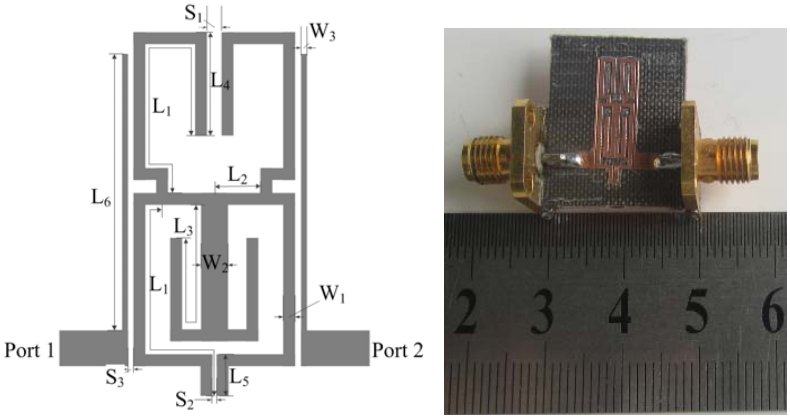

(a) (b)

Figure 6. The proposed wideband BPF. (a) Layout. (b) Photograph.

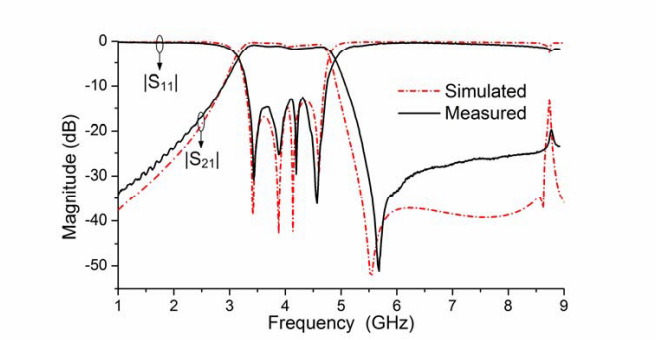

Figure 7. Simulated (line of short dash dot) and measured (solid line) results of the wideband BPF.

parameters of the BPF are optimized as follows: $W_1 = 0.5\,\text{mm}$, $W_2 = 1\,\text{mm}$, $W_3 = 0.2\,\text{mm}$, $S_1 = 0.5\,\text{mm}$, $S_2 = 0.22\,\text{mm}$, $S_3 = 0.22\,\text{mm}$, $L_1 = 12\,\text{mm}$, $L_2 = 0.8\,\text{mm}$, $L_3 = 11.5\,\text{mm}$, $L_4 = 5\,\text{mm}$, $L_5 = 2.2\,\text{mm}$, $L_6 = 13.2\,\text{mm}$. Simulated and measured frequency responses are compared in Figure 7. The measured 3-dB fractional bandwidth (FBW) for the passband centered at 4 GHz is found to be 3.1 GHz–4.9 GHz (45%). The measured passband return losses at all bands are below 14 dB, while the insertion loss of the passband is approximately 1.4 dB at 4.15 GHz. A transmission zero appears at 5.68 GHz, resulting in high selectivity. Finally, Table 1 compares the proposed filter with several reported wideband BPFs, where it illustrates the merits of this work about good passband performance and ultra compact size.

Table 1.

Ref.	Substrare Height/ε_r	3 dB FBW	Center Frequency	Insertion Loss	Return Loss	Size (λ_g*λ_g)
[1]	0.508 mm/2.2	51%	8 GHz	1.4 dB	15 dB	0.81 × 0.52
[2]	1 mm/2.65	69.2%	3.98 GHz	0.9 dB	15 dB	0.34 × 0.12
[3]	1 mm/2.65	69.1%	2.3 GHz	1 dB	20 dB	0.51 × 0.33
[4]	0.813 mm/3.38	107%	3.03 GHz	2.1 dB	11.7 dB	0.89 × 0.46
[5]	0.508 mm/2.2	48%	8 GHz	1.6 dB	15 dB	2.4 × 0.65
[6]	0.787 mm/2.2	52%	4.2 GHz	1.2 dB	20 dB	0.6 × 0.28
[7]	1 mm/2.45	88%	3.8 GHz	1.5 dB	12.2 dB	0.7 × 0.38
[8]	0.635 mm/10.8	64%	4.2 GHz	0.7 dB	20.0 dB	0.5 × 0.5
[9]	0.508 mm/3.38	45%	5.15 GHz	1.2 dB	20 dB	0.92 × 0.33
[12]	1 mm/2.2	37%	2.2 GHz	0.5 dB	22 dB	0.21 × 0.2
This work	**0.8 mm/2.55**	**45%**	**4 GHz**	**1.4 dB**	**14 dB**	**0.3 × 0.1**

4. CONCLUSION

An ultra compact wideband bandpass filter using a quadmode stub-loaded resonator is introduced in this letter. The first four modes of the proposed resonator can be freely adjusted. The filter has a simple design procedure. Measured results are in good agreement with the simulated ones and reveal low insertion loss, good return loss, and sharp out-of-band rejection skirts. Finally, the proposed compact wideband BPF is particularly suitable for wideband applications in communication systems.

ACKNOWLEDGMENT

This work was supported in part by the National Natural Science Foundation of China, (No. 61461020, U1431110), in part by the Science and Technology Project of Jiangxi Province Education Department (No. GJJ160752), in part by the Doctoral Scientific Research Foundation of Jinggangshan University (No. JZB17001).

REFERENCES

1. Hsu, C. L., F. C. Hsu, and J. T. Kuo, "Microstrip bandpass filter for ultra-wideband (UWB) wireless communications," *IEEE MTT-S Int. Dig.*, 679–682, Jun. 2005.
2. Deng, K., J. Z. Chen, S. J. Sun, B. Wu, and C.-H. Liang, "Microstrip wideband bandpass filter based on square ring loaded resonator," *Progress In Electromagnetics Research Letters*, Vol. 43, 175–184, 2013.
3. Li, Z. P., T. Su, and C. H. Liang, "Wide passband/stopband bandpass filter based on transversal signal interference concepts and modified branch-line structure," *Int. J. RF/Microwave Comp.-Aided. Eng.*, Vol. 25, No. 4, 330–336, 2015.
4. Li, Y., W. W. Choi, K. W. Tam, and L. Zhu, "Novel wideband bandpass filter with dual notched bands using stub-loaded resonators," *IEEE Microwave and Wireless Components Letters*, Vol. 27, No. 1, 25–27, 2017.
5. Chiou, Y. C., J. T. Kuo, and E. Cheng, "Broadband quasi-Chebyshev bandpass filters with multimode stepped-impedance resonators (SIRs)," *IEEE Transactions on Microwave Theory and Techniques*, Vol. 54, No. 8, 3352–3358, 2006.
6. Chang, Y. C., C. H. Kao, and M. H. Weng, "A compact wideband bandpass filter using single asymmetric SIR with low loss and high selectivity," *Microwave and Optical Technology Letters*, Vol. 51, No. 1, 242–244, 2009.
7. Nan, L., Y. Wu, W. Wang, S. Li, and Y. Liu, "A compact wideband bandpass filter using a coupled-line quad-mode resonator," *Progress In Electromagnetics Research Letters*, Vol. 53, 7–12, 2015.
8. Sun, S. and L. Zhu, "Wideband microstrip ring resonator bandpass filters under multiple resonances," *IEEE Transactions on Microwave Theory and Techniques*, Vol. 55, No. 10, 2176–2188, 2007.
9. Ma, K., K. Liang, R. M. Jayasuriya, and K. S. Yeo, "A wideband and high rejection multimode bandpass filter using stub perturbation," *IEEE Microwave and Wireless Components Letters*, Vol. 19, No. 1, 24–26, 2009.
10. Bo, J., L. Zhu, and D. Chen, "A novel wideband bandpass filter using triple-mode slotline ring resonator," *Progress In Electromagnetics Research Letters*, Vol. 40, 163–170, 2013.
11. Deng, H.-W., Y.-J. Zhao, L. Zhang, X.-S. Zhang, and W. Zhao, "Compact wideband bandpass filter with quadruple-mode stub-loaded resonator," *Progress In Electromagnetics Research Letters*, Vol. 17, 125–132, 2010.
12. Wei, F., Y. J. Guo, P.-Y. Qin, and X. W. Shi, "Wideband bandpass filter with a broad stopband based on a triple-mode stub-loaded resonator," *Microwave and Optical Technology Letters*, Vol. 56, No. 12, 2878–2881, 2014.
13. Wei, F. and X. W. Shi, "Compact quad-band BPF based on stub loaded double-ring resonator," *Microwave and Optical Technology Letters*, Vol. 56, No. 7, 1633–1635, 2014.